Interaction of 4-Hydroxybiphenyl with Cyclodextrins: Effect of Complex Structure on Spectroscopic and Photophysical Properties

Pietro Bortolus,*[a] Giancarlo Marconi,[a] Sandra Monti,[a] Bernd Mayer,*[b] Gottfried Köhler,[b] and Gottfried Grabner[b]

Abstract: The structures, spectroscopic and photophysical properties of the inclusion complexes between 4-OH-biphenyl and cyclodextrins (CD) in water were studied theoretically and experimentally. The complex structures were predicted using a dynamic Monte Carlo procedure including solvation effects and analyzed via computed and experimentally determined circular dichroism. The interpretation of the induced circular dichroism spectra indicated the formation of stable 2:2 complexes between the probe and α-CD, while 1:1 structures account for the circular dichroism induced by β- and γ-CD. Fluorescence emission quantum yields and lifetimes, measured as a function of the CD concentration, confirmed the formation of this higher order complex with α-CD. Prototropic equilibration in the singlet excited state was found to be depressed in 2:2 complexes due to the hydrophobic environment of the OH groups, while it remained unperturbed in 1:1 complexes, where the substituent is exposed to the aqueous environment. Triplet–triplet absorption and triplet quenching data supported this interpretation. The photophysical properties of both the 1:1 and the 2:2 complexes are characterized by a significant reduction of the nonradiative decay rates.

Keywords: circular dichroism · cyclodextrins · photophysics · structure elucidation

Introduction

Cyclodextrins (CDs) are water-soluble cyclic oligosaccharides formed by six (α-CD), seven (β-CD), and eight (γ-CD) glucopyranose units arranged in a toroidal shape, constituting a hydrophobic cavity. The aqueous solutions of CDs form inclusion complexes with a large variety of molecules.[1] The 1:1 and 1:2 (guest:host) complexes are the most common types of interactions,[2–4] but complexes with the stoichiometries 2:1,[5] 2:2,[6] and 1:3,[7] and even tubular assemblies,[8] have also been reported.

The spectroscopic and photochemical characteristics of an aromatic guest can be strongly modified by its inclusion in a CD cavity;[3, 4, 9] the variations depend on the nature of the CD, on the stoichiometry of the complexes, and on the mode of inclusion of the guest in the host cavity. For instance, the excited-state deprotonation rates of carbazole[10] and 1-NH_3^+-pyrene[11] are increased by inclusion in β- and γ-CD. On the contrary, the singlet excited states of 1- and 2-naphthol become less acidic upon CD-complexation.[12] In the case of α-CD as host, the excited-state deprotonation of 2-naphthol is suppressed by the formation of a 1:2 complex whose geometry was described by molecular mechanics modeling.[12c] In phenols with multiple methyl substitution, a marked decrease of the radiationless S_1-S_0 internal conversion and of the hydrated electron formation efficiency were observed,[13] while the photochemistry of phenol and *p*-cresol was only weakly affected by CD. This behavior was rationalized in terms of the complex structure and location of the phenolic OH group in the hydrophobic interior or in proximity of the "alcoholic" rim of the CD.

Compared with *p*-cresol, 4-hydroxy-biphenyl (B-OH) bears a hydrophobic, bulkier, phenyl group in *para*-position to the phenolic OH which makes this molecule a "bichromophoric" probe regarding its interactions with the CD cavity. Considering a 1:1 stoichiometry, two geometries could be envisaged for the complex: one with the phenyl included, the other with the phenol embedded in the cavity. The mode of inclusion should affect the prototropic equilibrium undergone by B-OH in the first excited singlet state.[14] Moreover, B-OH is an especially interesting probe for a study of the influence of the restricted environment of the CD cavity on the molecular motions. In fact, the biphenyl derivatives are in a twisted conformation in the ground state, the two phenyl rings forming a $\approx 40^\circ$ dihedral angle; this is reflected by the fact

[a] Dr. P. Bortolus, G. Marconi, S. Monti
Istituto di Fotochimica e Radiazioni d'Alta Energia
CNR Area della Ricerca, Via Piero Gobetti 101
40129 Bologna (Italy)
Fax: (+39) 051 639 9844
E-mail: monti@frae.bo.cnr.it

[b] Dr. B. Mayer, G. Köhler, G. Grabner
Institut für Theoretische Chemie und Strahlenchemie
University of Vienna, Althanstrasse 14
1090 Vienna (Austria)
Fax: (+43) 1 31336 790;
E-mail: bernd@asterix.msp.univie.ac.at

0947-6539/00/0609-1578 $ 17.50+.50/0 *Chem. Eur. J.* **2000**, *6*, No. 9

that their absorption bands are found at energies higher than those of the corresponding planar fluorenes.[15–17] The conformation becomes more planar following excitation to the first excited singlet state.[18] This change of geometry is expected to be influenced by the inclusion of the B-OH in the cavity, thereby affecting the deactivation channels of the excited probe. In this respect, it has been reported that the room temperature phosphorescence emission of B-OH adsorbed on α-CD/NaCl mixtures is affected by the cyclodextrin percentage. An increase of α-CD in the mixture from 0.05% to 80% increased the phosphorescence yield and lifetime. The variation was attributed to a higher rigidity of B-OH in the α-CD rich mixtures, possibly related to different modes of inclusion of the probe in the cavity.[19]

In the present work, the interaction of B-OH with α-, β-, and γ-CD was studied by spectroscopic (fluorescence and induced circular dichroism) and time resolved (fluorescence and triplet absorption) techniques both in acidic and in basic medium. The interactions of the neutral molecule with α- and β-CD were explored by a dynamic Monte Carlo (DMC) approach including solvation effects. The spectroscopic and photophysical behavior was interpreted in light of the obtained structural information.

Experimental Section

B-OH (Aldrich, sublimed 99%), α- and β-CD (Serva), and γ-CD (Aldrich) were used as received. Water was purified by passage through a Millipore MilliQ system. B-OH aqueous solutions were obtained by direct dissolution under stirring for 24 h. The obtained solution was filtered and diluted to the needed concentration. Steady-state and time-resolved fluorescence measurements were done in 1M HCl, 0.5M phosphate buffer (pH 11.2) and in 0.05M phosphate buffer, pH 6.76.

Ultraviolet absorption spectra were recorded on a Perkin–Elmer 320 spectrophotometer. Circular dichroism spectra were obtained with a Jasco J-710 dichrograph. Steady-state emission spectra were obtained by a Perkin–Elmer MPF 44 fluorimeter equipped with an accessory for spectral correction. Absorption and fluorescence experiments were carried out in cells thermostated at $\pm 1\,^{\circ}C$. Fluorescence emission spectra of B-OH and B-OH/CD solutions were obtained by exciting at the long-wavelength isosbestic point in the absorption spectrum (if present) or at a wavelength at which the difference in optical density between B-OH and B-OH/CD was minimal. The absorbance of the solutions was in all cases below 0.1. Fluorescence lifetimes were determined in air-saturated solutions by means of a time-correlated single photon counting system (IBH Consultants Ltd.). The hydrogen-filled nanosecond flashlamp was thyratron-driven at 40 kHz; the instrumental response function had a full width at half maximum of 2 ns. Fluorescence decays were treated by means of a software package provided by IBH Consultants Ltd. Decay functions including up to three exponential components were fitted to the emission signals by deconvolution of the instrumental response via a non-linear procedure based on a least-squares method. Global analysis of decays taken at different wavelengths was performed. Distribution of residuals, Durbin–Watson parameter, and χ^2 were used to evaluate the quality of the fit.

Transient absorption spectroscopy was carried out using the fourth harmonic of a Nd/YAG laser (Quanta-Ray DCR-1) as the excitation source. Details of the experimental setup and of the measurements procedures have been published earlier.[20]

Theoretical Methods

Calculation of low energy complex structures: The computation of the potential energies of 1:1, 1:2 and 2:2 CD:BOH complex geometries was based on Allinger's MM3-92 force field applying a block diagonal matrix minimization method.[21] The fully minimized reference structures of α- and β-CD, derived from crystallographic data,[22] show an energy of 257 kJ mol^{-1} and 298 kJ mol^{-1}, respectively, while the potential energy of the B-OH guest results as 36 kJ mol^{-1}. Starting from these reference structures, low energy complex geometries were searched by applying a dynamic Monte Carlo (DMC) routine[23] within the program package MultiMize.[24] Both the potential energies (calculated by the force field) and the solvation effects (calculated by a continuum approximation assigning atomic solvation parameters to the solvent accessible molecular surface area) were considered in a modified Metropolis criterion. Details of the calculation have been reported earlier.[25] This method, which combines the potential energies calculated by a force field and the free energies of solvation derived from a continuum approximation, proved to give valuable structural results for CD complexes in aqueous environments.[25–27] The contributions arising from solvation effects, here mainly hydrophobic interactions, were found to be an important prerequisite to obtain correct complex geometries.[25]

The start geometries for DMC runs were defined by a random relative orientation of host and guest within a distance of 5 Å. In each DMC step the relative position was stochastically altered in x, y and z axis by a maximum of 0.5 Å, the guest was rotated by a maximum of 5°, and the individual glucose units within the CD were also rotated by a maximum of 5°. Each stochastically generated structure was fully minimized within the force field and accepted according to the modified Metropolis criterion.[25] The simulation temperature was kept constant at 300 K and low energy complex structures were obtained within 1000 DMC steps. The complexes are characterized by the potential energies E_{pot} (in kJ mol^{-1}) and by a host:guest distance d (in Å), defined by the distance between the center of mass of the guest and the mean position of the glycosidic oxygens of the macrocycle. Furthermore a complexation energy ΔE (in kJ mol^{-1}) is provided as the difference between the calculated complex energy and the sum of the potential energies of the isolated host and guest molecules.

Calculation of the icd spectra: In order to test the reliability of the determined geometries, a calculation of the induced circular dichroism (icd) was carried out for the generated energy minima. In the case of 1:1 or 1:2 complexes, the rotational strength arises from the interaction of the dipole transition moments of the guest excited states with those (at high energy) of the macrocycle. The pertinent expression is obtained by replacing the original dipole–dipole interaction scheme[28] in the Kirkwood equations by the polarizability of the bonds of the chiral macrocycle. According to this approximation, the equations of the rotatory strength for a transition $0 \rightarrow a$ are given by

$$R_{0a} = \pi \nu_a \mu_{0a}^2 \sum_j \frac{\nu_{0j}^2 \, (\alpha_{33} - \alpha_{11})_j \, (GF)_j}{c \, (\nu_{0j}^2 - \nu_a^2)} \qquad (1)$$

where $\boldsymbol{e}_{0a}$ and $\boldsymbol{e}_j$ are unit vectors along the transition moment μ_{0a} and parallel to the j-th bond, respectively; ν_{0j} and ν_a are the

frequencies of the electric transitions of the host and the guest located at a distance $\mathbf{r}_j$; α_{11} and α_{33} represent the bond polarizabilities at zero frequency, parallel and perpendicular to the symmetry axis of the bond j. In Equation (2) the energies and electric moments were calculated by using a semiempirical quantum mechanical method (CNDO/S).

$$(GF)_j = \frac{1}{r_j^3}\left[\boldsymbol{e}_{0a}\boldsymbol{e}_j - \frac{3\,(e_{0a}r_j)\,(e_jr_j)}{r_j^2}\right]\boldsymbol{e}_{0a}\times\boldsymbol{e}_j\boldsymbol{r}_j \qquad (2)$$

In the case of 2:2 complexes, an explicit interaction between the electric dipole transition moments of two B-OH molecules has to be considered and a term derived from the dimer model (Moffit exciton coupling) has to be added to Equation (2):[29]

$$\boldsymbol{R}_{0a}^{d} = \pm(\pi/2\lambda)\boldsymbol{R}_{12}\langle\varphi_{20}\,|\,\mu_2\,|\,\varphi_{2a}\rangle\times\langle\varphi_{10}\,|\,\mu_1\,|\,\varphi_{1a}\rangle \qquad (3)$$

This term, which is responsible for a characteristic sigmoidal shape of the spectrum, with the zero point corresponding to the maximum of the absorption band, can be the dominant one (depending on the concentration of the 2:2 complex) and can provide an immediate diagnosis of the presence of higher order complexes. Finally, for weakly allowed states it can be important to add also the $m-\mu$ term, arising from the interaction of a magnetic dipole term of a state with the electric dipole moments of the other states.[28, 29]

Results and Discussion

Absorption spectra: The absorption spectrum of B-OH ($c = 3.09\times10^{-5}$ M) in phosphate buffer, pH 6.76, and in 1M HCl is characterized by a structureless band ($\lambda_{max} = 258$ nm, $\varepsilon_{max} = 19\,000\,M^{-1}cm^{-1}$). In phosphate buffer, pH 11.2, the spectrum remains unstructured and shifts to the red ($\lambda_{max} = 287$ nm, $\varepsilon_{max} = 21\,500\,M^{-1}cm^{-1}$) owing to the deprotonation of B-OH. We found a pK_a 9.78 at 22 °C by pH titration in phosphate buffer (0.05 M) using absorption and fluorescence. This value should be compared with pK_a 9.56 reported in the literature[14]. The value of pK_a increased to 10.25, 10.00, and 10.06 in presence of 10^{-2} M α-, β-, and γ-CD, respectively. In both media the band is attributed to the $^1L_a \leftarrow {}^1A$ transition which hides the much less intense $^1L_b \leftarrow {}^1A$ transition.[14] At higher energies the spectrum has a very intense band due to the $^1B_b \leftarrow {}^1A$ transition centered at ≈210 nm.

Addition of 5.12×10^{-2} M α-CD to a phosphate solution or to a 1M HCl solution of B-OH caused a loss of the intensity of the above-mentioned band and left the value of λ_{max} unaltered. The tail of the band was shifted to the red by ≈1 nm and strong variations both in intensity and in the wavelength of the onset were observed for the higher-energy transition. Similar variations were observed after addition of 1.05×10^{-2} M β-CD (Figure 1) or 2×10^{-2} M γ-CD. In alkaline solution (pH 11.2, phosphate buffer) all the CDs caused a loss of intensity of the low-energy band whose λ_{max} (287 nm) remained unaltered in the presence of α-CD and shifted to 289–290 nm in the presence of β- and γ-CD. The high-energy band, instead, remained unaffected.

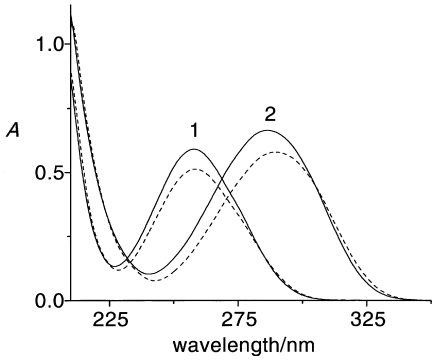

Figure 1. Absorption spectra of 4-hydroxybiphenyl 3.09×10^{-5} M: in phosphate buffer 0.05 M 1) pH 6.76, 2) pH 11.2, alone (——) and in presence of 1.05×10^{-2} M β-CD (- - - -). Cell path 1 cm, $T = 295$ K.

On the basis of these spectral changes, we argue that both B-OH and its ionized form interact with the three CDs and that their ground state conformation is not noticeably affected by the interaction.

Induced circular dichroism spectra: Induced circular dichroism (icd) was observed in B-OH by CD complexation in neutral and 1M HCl solutions. The addition of α-CD induced a positive signal below 210 nm, a narrow negative band with a peak at ≈222 nm, a large positive band with maximum at ≈253 nm, and a weak negative signal around 295 nm. The icd spectrum shown in Figure 2 has maxima/minima which do not

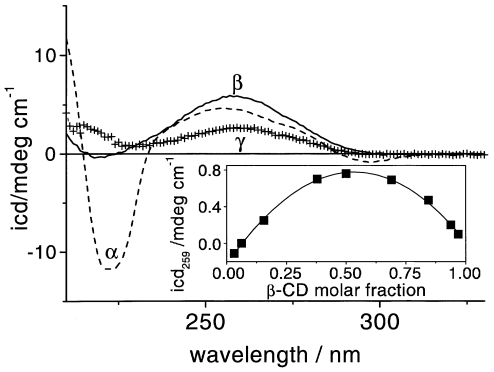

Figure 2. Circular dichroism spectra of B-OH 4.74×10^{-5} M in 1M HCl in presence of α-CD 5.0×10^{-2} M (– – –), β-CD 3.0×10^{-3} M (——), γ-CD 1.1×10^{-2} M (+ + +). Cell path 1 cm, $T = 295$ K. Inset: Job plot of the icd signal of B-OH at 259 nm in presence of β-CD. Total concentration 8.7×10^{-5} M.

coincide with those of the corresponding absorption spectrum. This suggests that an exciton splitting of the dichroic bands occurs and indicates that an inclusion complex where two B-OH molecules strongly interact with each other is formed in the cyclodextrin environment. Further experimental results as well as the conformational calculations confirm this view (see below).

In the presence of β-CD, the icd spectrum showed two positive bands peaking at 200 and 258 nm, which correspond to the bands in the absorption spectrum, at both neutral pH and in 1M HCl. No evidence for any exciton splitting was found, except for a very weak negative signal at ≈220 nm. The Job plot[30] shown in Figure 2 exhibits a maximum at 0.5 molar

0947-6539/00/0609-1580 $ 17.50+.50/0 *Chem. Eur. J.* **2000**, *6*, No. 9

fraction of β-CD. This result is consistent with a 1:1 or 2:2 stoichiometry of the complex and with coexistence of the two complex types in solution. However, the dependence of the icd signal intensity at 258 nm on the [β-CD] is best accounted for by the formation of a complex with stoichiometry 1:1 and an association constant, $K = 3500\,\text{M}^{-1}$ at 22 °C. Apparently the 2:2 structure, theoretically predicted as strongly favored, is not present in significant concentrations in our experimental conditions. On the basis of the results of the global analysis of the time-resolved fluorescence emission (see infra) it is inferred that such a complex may be present as a minor component. In the presence of γ-CD, the icd signal is constituted by two positive bands with maximum at ca. 210 and 260 nm at both neutral pH and in 1M HCl.

At pH 11.2 (0.5M phosphate buffer), the icd signal with α-CD was negative below 225 nm and three positive bands with maxima at 230, 255, and 315 nm were observed (Figure 3). The spectrum has a similar appearance in 0.1M NaOH. It can therefore be safely concluded that at pH 11.2 the icd signal is mainly shaped by the complexation of the anionic form, B-O$^-$, despite a fraction of $\approx$13% of B-OH molecules which are undissociated. Moreover, the fact that $\approx$10% of the CD hydroxyl groups are dissociated (pK_a of CD $\approx$12.1[31]) does not noticeably affect the results. In presence of β-CD, the icd signal has a positive band peaking at 280 nm and is negative below 240 nm. A good correspondence between the UV and icd absorption maxima was found. In the presence of γ-CD, the signal is positive in the whole range and the maximum of the lowest energy band also coincides with that of the absorption.

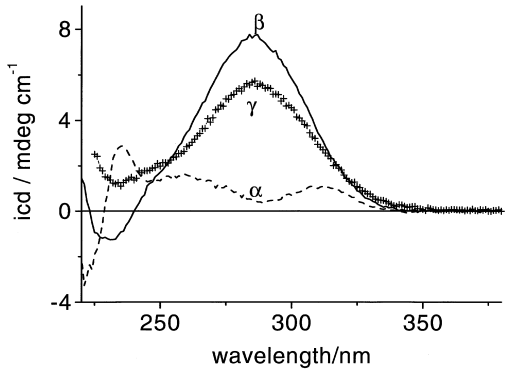

Figure 3. Circular dichroism spectra of B-O$^-$ 5.40×10^{-5}M in 0.5M phospate buffer pH 11.2 in presence of α-CD 5.0×10^{-2}M (– – –), β-CD 7.2×10^{-3}M (——), γ-CD 2.3×10^{-2}M (+ + +). Cell path 1 cm, $T = 295$ K.

Conformational calculations: The main results of the conformational calculations are presented in Table 1 and displayed in Figures 4–6. In general, the inclusion of B-OH in cyclodextrins is energetically feasible for all the types of complexes considered. However, the specific structural and, consequently, the spectroscopic properties, show significant differences that can be summarized as follows.

1:1 Complexes: Figure 4 shows the 1:1 complexes between B-OH and α- and β-CD, respectively. In the complex with α-CD, the guest is only attached to the secondary hydroxyl rim

Table 1. Calculated complexation energies for low energy complexes of B-OH with cyclodextrins.

CD	Type of complex	ΔE (kJ mol^{-1})
α	1:1	– 83.6
β	1:1	– 76.9
α	1:2	– 98.2
β	1:2	– 301.0
α	2:2 B geometry	– 242.9
α	2:2 C geometry	– 233.2
α	2:2 A geometry	– 228.2
β	2:2 A geometry	– 539.2
β	2:2 C geometry	– 413.8
β	2:2 B geometry	– 387.9

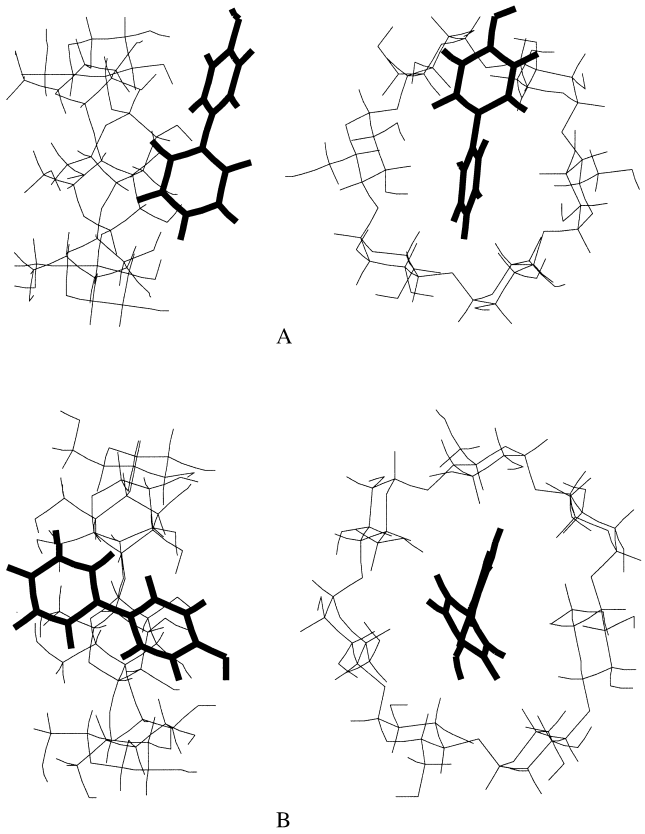

Figure 4. Computed conformations of 1:1 complexes of α-CD A) and β-CD B) with B-OH.

side, a feature which is reflected by a large host:guest distance of $\approx$5 Å. Axial inclusion of the phenyl ring results in an energy increase of $\approx$9 kJ mol^{-1} due to steric constraints within the deformed α-CD. The OH group of the guest is fully exposed to the solvent thus enabling the formation of an intermolecular hydrogen bond with a water molecule outside the cavity.

In the low-energy complex with β-CD, one ring of the guest is fully embedded in the macrocycle cavity (host:guest distance of 1.9 Å) but the OH group is exposed to the solvent outside the ring. The large cavity of β-CD prevents a tight fit with the aromatic ring (central position) resulting in a considerable overall flexibility of the complex.

The icd contribution arising from this kind of 1:1 complexation consists of three positive signals corresponding to the

three lowest excited singlets calculated at 276 nm ($f=0.04$), 270 nm ($f=0.35$), 205 nm ($f=0.7$) and with a rotational strength of 0.14, 1.32, and 29.75×10^{-39} c.g.s. for the β-CD inclusion and 0.21, 2.04, 4.62×10^{-39} c.g.s. for the β inclusion, respectively. By using the relationship:[32]

$$R=0.696\times10^{-42}\pi^{1/2}[\theta_{max}]\Delta\theta/\lambda_{max} \quad (4)$$

a value of $R=1.83\times10^{-39}$ c.g.s. can be determined for the first sizeable band from the icd spectrum of the β-CD complex, in good agreement with the calculated value of 2.04×10^{-39} c.g.s. This constitutes a valid test for the hypothesis that the 1:1 type of complexation is the dominant one in this case (see below).

1:2 Complexes: The formation of a complex between one molecule of B-OH and two α-CD molecules was not supported by the results of the calculations. The start geometry for the DMC run is defined by a guest residing in between the two host molecules. The guest remains in an axial position, but the phenyl ring is not embedded in the cavity. The OH group on the second ring virtually prevents the association of the other CD molecule with the first host. This situation hinders the formation of stable 1:2 complexes as intermolecular hydrogen bonding between the CDs, a prerequisite for stable 1:2 complexes, does not occur.

This picture changes substantially in 1:2 complexes with β-CD. The two CD molecules form a tight, hydrogen bonded associate fully encapsulating the guest molecule. The unfavorable energetic contribution of the OH group in the center of a CD cavity is counteracted by the enthalpic contribution of hydrogen-bond formation between the hosts.

The icd calculations give results analogous to the 1:1 complexation, that is, three positive bands in both cases, but with a larger value, due to the additive interaction of the chromophore with the states of two macrocycle units (e.g., for the β-CD 1:2 complex, $R=3.38\times10^{-39}$ c.g.s. for the second state). Significant formation of a 1:2 complex with β-CD was, however, excluded on the basis of the Job plot (Figure 2) and of the fluorescence results (see below).

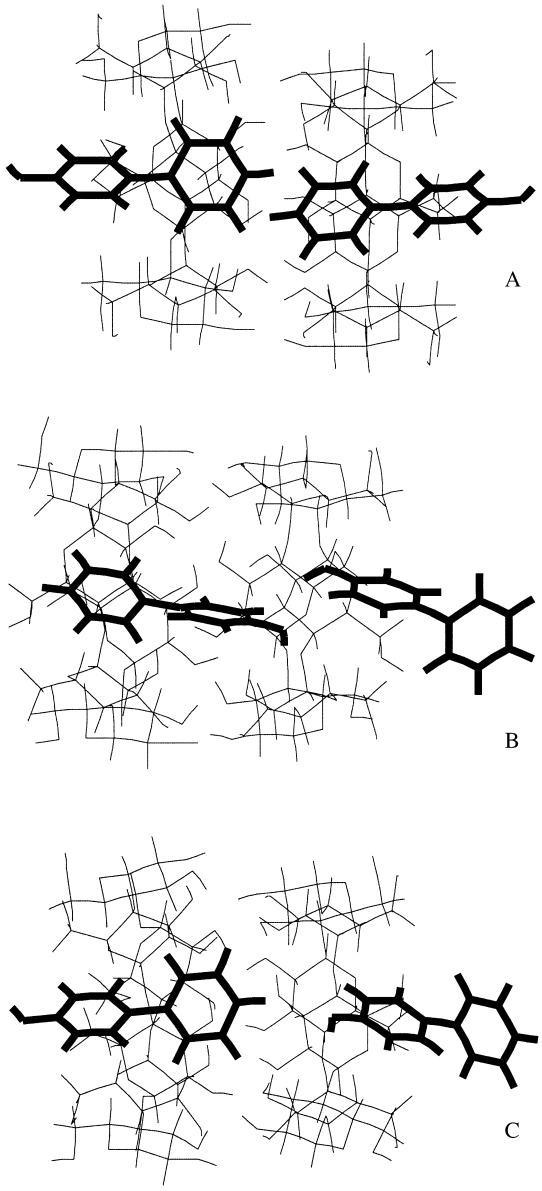

Figure 5. Computed conformations of 2:2 complexes of α-CD with B-OH: A) $\Delta E=-228.2$ kJ mol^{-1}, B) $\Delta E=-242.9$ kJ mol^{-1}, C) $\Delta E=-233.2$ kJ mol^{-1}.

2:2 Complexes: Three different 2:2 complexes between B-OH and α-CD were considered. Interestingly, this type of higher order complex is very stable according to the DMC calculations. The optimization algorithm found comparable gains in complexation energy ΔE for all the three arrangements of the guest. This is astonishing in view of the essential differences of the structural features resulting from the arrangements of the guests. In fact, the geometry in Figure 5A gives a highly symmetric alignment of the guest molecules and also of the individual hosts. The deformation of the macrocycles resulting from the full inclusion of the phenyl ring is counteracted by the partial hydrogen-bond formation between the secondary hydroxyl rim sides of the hosts and partly by energetically beneficial interactions between the guests. The low energy of the arrangement shown in Figure 5B is surprising. Both hydroxyl groups of the guests are embedded in the CD cavities (never encountered in the 1:1 or 1:2 complexes), but this energetical disadvantage is counteracted by a perfect arrangement of the donor and acceptor moieties allowing the formation of intermolecular hydrogen bonds between the hosts. This higher order complex of symmetric type is not present in the situation shown in Figure 5C where the guest to the left is not embedded and the host to the right is considerably distorted so as to hinder effective intermolecular hydrogen bonding between the hosts.

In the comparable simulations on 2:2 B-OH complexes with β-CD, the three relative orientations of the guest result again in stable 2:2 complexes (see Figure 6A – C), but the structure A is highly preferred. In this case the CDs give the best possible hydrogen-bond matching, the guest molecules are fully included and show a partial stacking of the phenyl groups and the OH groups are situated right in the plane

  0947-6539/00/0609-1582 $ 17.50+.50/0 *Chem. Eur. J.* **2000**, *6*, No. 9

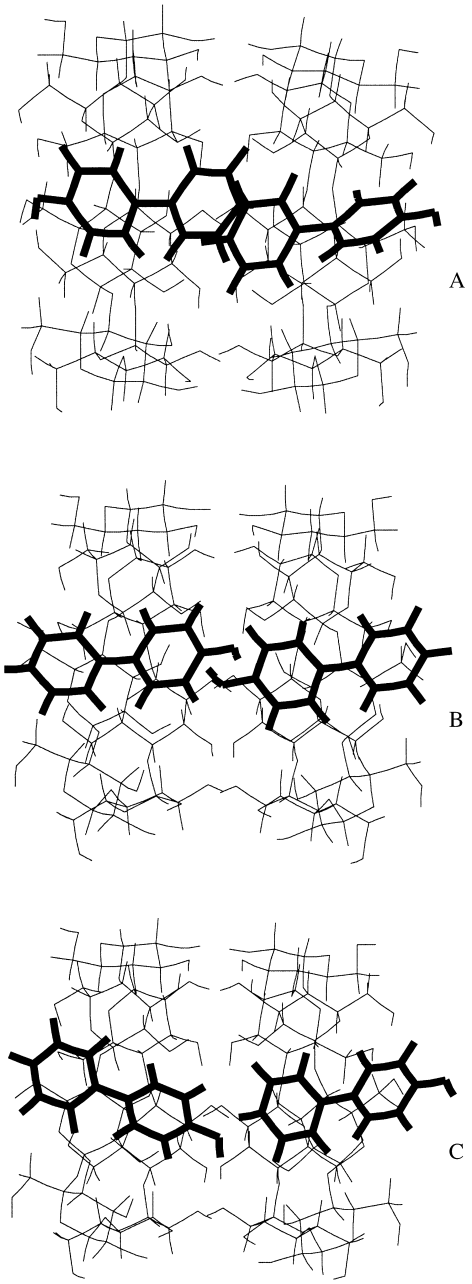

Figure 6. Computed conformations of 2:2 complexes of β-CD with B-OH: A) $\Delta E = -539.2$ kJ mol^{-1}, B) $\Delta E = -387.9$ kJ mol^{-1}, C) $\Delta E = -413.8$ kJ mol^{-1}.

defined by the secondary hydroxyl groups of the CD. This complex is characterized by a considerable stability and by a major change in the microenvironment of the guest molecules near the phenyl group and in proximity of the phenolic OH. This fact is expected to be strongly reflected in the photophysical properties of the complex.

In the case of higher order complexes, the icd calculation appears dominated by the exciton contribution given by Equation (3) for the allowed states and by the m-μ interaction for weakly allowed states such as the first singlet of B-OH. It is found that the exciton splitting gives rise to a contribution one order of magnitude larger with respect to the anisotropic interaction chromophore–cyclodextrin. Since the exciton contribution leads to a splitting of the bands with null rotational strength corresponding to the maximum of the absorption, we can interpret the icd spectrum in presence of α-CD as due to the splitting of the two sizeable absorption bands, that is $^1L_a \leftarrow {}^1A_g$ and $^1B_b \leftarrow {}^1A_g$. The conformation with the asymmetric facing of the phenol and phenyl moieties appears most consistent with the shape of the experimental spectrum. Figure 7 shows a typical sequence of bands calculated for a low energy conformation. The conformation

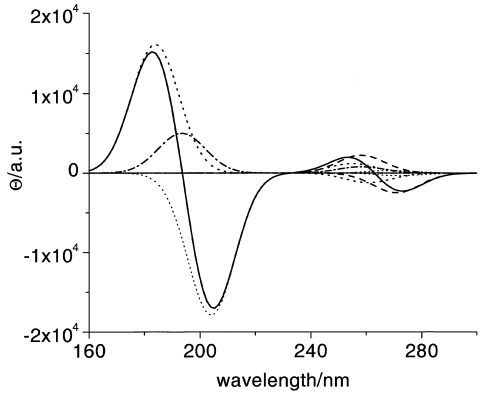

Figure 7. Calculated icd for the 2:2 complex of α-CD with B-OH in the C geometry. Exciton contribution (···), interaction chromophore–chiral macrocycle (•–•–), "m–μ" interaction (– – –), total resultant (——).

with the two phenyls faced gives rise to a very large exciton splitting that is not accounted for by the icd spectrum, while that with the two hydroxyl groups embedded and the two phenyl moieties protruding from the macrocycles appears much less favored on the basis of the calculated icd in spite of a slightly more favorable energy of complexation (see Table 1). In β-CD, the calculation produced a very strong exciton splitting signal especially for the phenyl-faced conformation. The very small signal experimentally detected in this system, with a negative peak at $\approx$220 nm, can therefore be taken as an indication of the contribution of a small amount of the 2:2 complex.

Fluorescence emission: The emission of B-OH in water consists of a structureless band with a maximum at 331–332 nm (hereafter called blue-band) with a long tail extending up to 560 nm. In phosphate buffer, pH 6.76, $[HPO_4]^{2-} = [H_2PO_4]^- = 0.05$ M, the tail evolved to a shoulder, while it disappeared in 1M HCl, suggesting that the long-wavelength emission (hereafter called red-band) is due to the presence of the anion of B-OH (B-O$^-$) formed by partial prototropic equilibration of the molecule in the excited state. This hypothesis is confirmed by the fluorescence decay which is well described by a linear combination of two exponentials terms with the time constants 3.0 and 0.95 ns and pre-exponentials factors positive at 335 nm and equal in absolute value but opposite in sign at 420 nm (see below). In phosphate buffer pH 11.2, the structureless emission of the dissociated B-O$^-$ had a band maximum at $\approx$400 nm. No influence of oxygen on the emission could be detected at any pH value.

Intensity measurements: The effect of the addition of the three CDs to a B-OH solution in 0.05 M phosphate buffer,

pH 6.76, is reported in Figure 8. This figure clearly shows that the emission intensity of the blue-band was enhanced by all the CDs, while the intensity of the red-band was enhanced by β- and γ-CD and depressed by α-CD; the λ_{max} of the blue-band was unaffected by the presence of the CDs. The changes

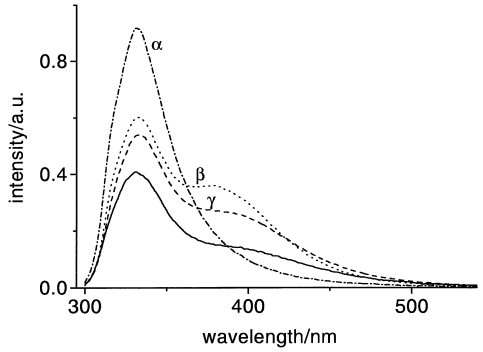

Figure 8. Fluorescence spectra of B-OH 2.2×10^{-5} M in phosphate buffer 0.05 M, pH 6.76: alone (——) and in presence of [β-CD] $= 2.0 \times 10^{-2}$ M (•–•–), [β-CD] $= 6.9 \times 10^{-3}$ M (···), [γ-CD] $= 2.0 \times 10^{-2}$ M (– – –). $T = 295$ K.

in the emission yields confirm the formation of inclusion complexes between B-OH in the ground state (at this pH the molecule is not appreciably dissociated) and the cyclodextrins; since the emission process occurs in a few nanoseconds, one can safely assume that the complexation equilibrium of the ground state does not change during the life of the emitting state. In contrast to what was reported for 4-biphenylcarboxylic acid,[32] whose fluorescence emission undergoes a $\approx$30 nm blue-shift upon addition of both α- and β-CD, no appreciable shift of the B-OH blue-band was induced by the addition of the CDs. The shift observed in 4-biphenylcarboxylic acid was attributed to an excited-state geometry change of the biphenyl moiety towards coplanarity, favored by the reduced polarity of the CD cavity.[32] One can conclude that the complexation does not modify the excited-state conformation of B-OH to the same extent.

Figure 9 shows the emission of a B-OH solution in 0.05 M phosphate buffer, pH 6.76, excited at the isosbestic point, 280 nm, upon addition of α-CD. After an initial, small decrease of the emission in the whole wavelength range, an increase of the intensity of the blue-band was observed concurrently with a decrease of the red-band due to B-O$^-$; a well-defined isoemissive point is present at 388 – 389 nm. The insert of Figure 9 reports the dependence of the anionic fluorescence on [α-CD]; the difference spectra shown were calculated using the spectrum obtained in 1 M HCl to normalize and subtract the blue-band from the emission at pH 6.76. These variations indicate that the formation of a complex between B-OH in the ground state and α-CD decreases the efficiency of proton dissociation from the guest in the singlet excited state. On the contrary, the formation of a complex between B-OH and β- or γ-CD does not prevent the establishment of the acid – base equilibration in the excited state, as indicated by the persistence of both the blue- and the red-band in the emission spectrum shown in Figure 8. At variance with the behavior of 2-naphthol, whose excited-state proton transfer is depressed by inclusion in the cavity of

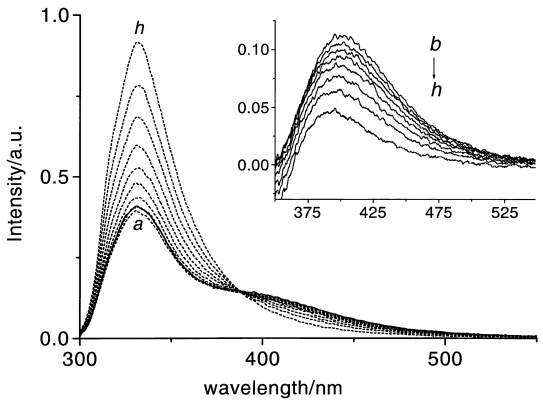

Figure 9. Variations of the fluorescence emission intensity from a solution of B-OH 2.2×10^{-5} M in phosphate buffer 0.05 M, pH 6.76 (——), upon addition of α-CD (– – –): *a*) 4.42×10^{-5} M, b) 9.93×10^{-4} M, c) 2.03×10^{-3} M, d) 4.13×10^{-3} M, e) 5.91×10^{-3} M, f) 8.44×10^{-3} M, g) 1.2×10^{-2} M, h) 2.01×10^{-2} M. $\lambda_{exc} = 280$ nm, isosbestic point, $T = 295$ K. Inset: decrease of the base emission with increasing α-CD concentration.

α- and β-CD,[12] only α-CD hampers this process in the case of B-OH.

The variations of the fluorescence emission due to the presence of α-CD indicate that the depression of the excited-state deprotonation is a two-step process. The first interaction between B-OH and α-CD leads to a small, but clearly observable and reproducible, reduction of the emission yield without any variation of the spectral distribution. The formation of a 1:1 complex, in which the phenolic OH group is fully exposed to the solvent and therefore able to participate in an acid – base equilibration, explains this behavior well. The structure of the 1:1 B-OH:α-CD complex predicted by the theoretical calculations and shown in Figure 4 is in agreement with the observed photophysical behavior. The increase of the blue-band, and the concurrent decrease of the red-band for [α-CD] $\geq 10^{-3}$ M indicates the formation of a structure in which the OH group of the probe is not fully exposed to the solvent and therefore its dissociation in the excited state is partially hampered. The formation of a 2:1 complex, like in the system α-CD:2-naphthol,[11c] or a large influence of the complexation on the pK_a* value could be suggested to explain the observed dependence of the fluorescence emission on [α-CD]. The first hypothesis is in disagreement with the icd spectra and with the results of the calculations which both suggest the formation of a structure in which two B-OH molecules interact. The negligible shift induced by the presence of cyclodextrins (10^{-2} M) on the absorption and emission spectra of both B-OH and its ionized form allows to safely assume that the influence of the complexation on pK_a* is similar to that on the pK_a of the ground state (Δp$K_a \approx 0.5$ units), so that the second hypothesis can be discarded too.

The fluorescence and icd data are therefore consistent with the sequential formation of 1:1 and 2:2 complexes, that is with the establishment of the following equilibria in solution:

$$\alpha\text{-CD} + \text{B-OH} \rightleftharpoons \alpha\text{-CD}\cdot\text{B-OH} \qquad K_1 \qquad (5)$$

$$2(\alpha\text{-CD}\cdot\text{B-OH}) \rightleftharpoons (\alpha\text{-CD}\cdot\text{B-OH})_2 \qquad K_2 \qquad (6)$$

0947-6539/00/0609-1584 $ 17.50+.50/0 *Chem. Eur. J.* **2000**, *6*, No. 9

If the concentration of α-CD can be considered as constant, the ratio of the integrated fluorescence intensities, F/F_0, where F_0 is the fluorescence in water and F that in presence of a given [α-CD], is expressed as follows:

$$F/F_0 = s+R_1K_1s[\alpha\text{-CD}]+R_2(1-s-K_1s[\alpha\text{-CD}]) \quad (7)$$

with

$$s = 1-[1{:}1]/c_0-[2{:}2]/c_0 \quad (8)$$

In Equation (7) s is the fraction of free B-OH molecules, $R_1=\Phi_1/\Phi_0$ and $R_2=\Phi_2/\Phi_0$, where Φ_0 is the fluorescence quantum yield of the free molecule, Φ_1 that of the 1:1 complex and Φ_2 that of the 2:2 complex. By expressing the concentrations of the 1:1 and 2:2 complexes in terms of the equilibrium constants, $K_1=[1{:}1]/(fc_0[\alpha\text{-CD}])$ and $K_2=[2{:}2]/[1{:}1]^2$, the four parameters R_1, R_2, K_1, and K_2 can in principle be determined by best fitting of the experimental F/F_0 values to Equation (7). Due to parameter correlation, the least-squares fitting procedure does not lead to a unique solution, so that definite values of the association constants and of the quantum yields of the emitting species cannot be given at this point. We shall see below that a consideration of the photophysical properties of the 2:2 complex allows an estimation of the complexation properties based on a reasonable assumption of the fluorescence quantum yield.

The fluorescence intensity variations induced by γ-CD are consistent with the formation of a 1:1 complex. The association constant K was obtained by best fitting of the experimental F/F_0 values to the Equation (9):

$$F/F_0 = \{1+K(\Phi_b/\Phi_0)[\gamma\text{-CD}]\}/(1+K[\gamma\text{-CD}]) \quad (9)$$

where Φ_b is the emission quantum yield of the 1:1 complex.[13] The large dimensions of the cavity, which can accomodate water molecules besides the guest, allow the acid–base equilibration in the excited state to occur; consequently, both the blue- and the red-band are present in the emission spectrum. The association constants obtained by nonlinear least-squares fitting are reported in Table 2.

The system β-CD:B-OH is the most elusive. The presence of both the blue- and the red-band indicates that the prototropic equilibration in the excited state still occurs. The fluorescence variations are satisfactorily accounted for by the formation of 1:1 complex for which the calculations indicate a structure with the phenyl ring fully embedded in the CD-cavity but the OH group exposed to the bulk water. However, the fluorescence intensity variations in the presence of β-CD can be accounted for also by the simultaneous presence of two emitting complexes of 1:1 and 2:2 stoichiometry, according to the scheme for the interaction of B-OH with α-CD proposed above. Again the model does not allow unequivocal quantitative conclusions to be reached for both association constants and emission quantum yields of the complexed species. The formation of a 2:2 structure is suggested by the temperature effect on the limiting F/F_o ratio which, from the value 2.17 at 13.5 °C, steadily increases up to 2.59 at 51.5 °C, indicating that two species with fluorescence yields higher than that of the free molecule are simultaneously present in solution. A 2:2 structure with the phenolic OH partially exposed to the outer solvent is in agreement with the results of the conformational calculations but its equilibrium concentration is probably very low as indicated by the icd spectra and by the fluorescence decay data (see below).

In view of the analysis of B-OH:CD system by time-resolved experiments, the variations of the fluorescence emission intensity by addition of CDs were also determined in 1M HCl solution. In this medium, the acid–base equilibration of B-OH in the singlet excited state is suppressed[14] and it is reasonable to assume that this holds true both for the free and the complexed species. This simplifies the analysis of the decay profiles. In Figure 10, the dependence of the ratio F/F_0 on the concentration of the three CDs in the acidic medium is reported. The shape of the curves and the main conclusions of

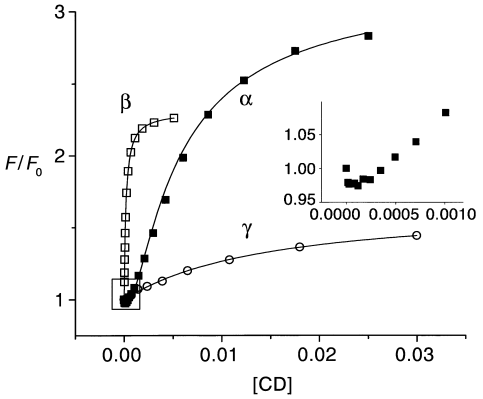

Figure 10. Dependence of the fluorescence emission intensity of B-OH 2.2×10^{-5} M in 1M HCl, $\lambda_{exc}=280$ nm, on the α-, β-, and γ-CD concentration. The continuous lines represent best fits to Equation (7) for α-CD ($R_1=0.08$, $R_2=5.5$ (fixed), $K_1=118\,M^{-1}$, $K_2=75000\,M^{-1}$ (fixed) and to Equation (9) for β-CD ($R=2.45$, $K=5500\,M^{-1}$) and γ-CD ($R=1.66$, $K=66\,M^{-1}$). $T=295$ K. Inset: zoom in the α-CD plot.

Table 2. Association constants K and emission quantum yield ratios $R=\varphi_b/\Phi_0$ for the complexes of 4-hydroxybiphenyl extracted by best fitting of the fluorescence intensity plots to Equation (9) for β- and γ-CD and to Equation (7) for α-CD.

	1M HCl		pH 11.2	
	K/M^{-1}[a]	Φ_b[a]/Φ_0	K/M^{-1}[a]	Φ_b[a]/Φ_0
β-CD (1:1)	5500	2.45	6000	2.8
γ-CD (1:1)	66	1.7	150	2.4
α-CD (1:1)	(120)[b]	(0.1)[b]	65	1.5
α-CD (2:2)	75000[c]	5.5[c]		

[a] Estimated uncertainties on K within ±15%, on R within ±10%. [b] This value is only indicative since it is not well defined by best fitting based on Eq. (7), see text. [c] This value was fixed in Eq. (7), see text.

the best fitting procedures are the same as those obtained in phosphate buffer (pH 6.76). The fluorescence intensity first decreases and then increases in the presence of increasing [α-CD] and monotonically increases with increasing [β-CD], and [γ-CD]. The fluorescence variations clearly indicate the existence of a two-step process for the complexation of B-OH with γ-CD, the formation of 1:1 complex with γ-CD, and the predominant presence of a 1:1 complex with β-CD. The best fitting curves to Equation (9) are shown for β- and γ-

CD and the relevant parameters are reported in Table 2. As we have already noticed, the determination of the association constants and emission quantum yield ratios by best fitting of the dependence of the fluorescence intensity on [α-CD] according to Equation (7) is not unequivocal. The fit, compatible with the experimental results, reported in Figure 10 was obtained by fixing the parameters relevant to the 2:2 complex to reproduce the plateau region. In the section on the photophysical parameters these assumptions and their consequences will be discussed.

The study of the complexation of the anion B-O$^-$ was carried out in 0.5 M phosphate buffer, pH 11.2. This pH represents a compromise between two contrasting requirements, avoiding the presence of appreciable amounts of ionized cyclodextrins, p$K_a \approx 12.1$, on the one hand, and that of appreciable amounts of undissociated B-OH, pK_a 9.78, on the other. In the presence of cyclodextrins, α-CD in particular, the value of pK_a is increased (see above) and therefore the excitation wavelength was set at 310 nm to reduce the drawbacks due to the presence of undissociated B-OH. The integrated emission was corrected for the optical density variations induced by the complexation. The addition of CDs to the solutions induces a blue-shift of the emission ($\approx$10 nm in presence of 10^{-2} M β-CD and $\approx$5 nm in presence of 3×10^{-2} M α-CD) and an increase of the B-O$^-$ fluorescence yield which is well described by the Equation (9). This indicates that B-O$^-$ forms inclusion complexes of 1:1 stoichiometry with the three cyclodextrins, in agreement with the results of the icd experiments. Molecular calculations cannot help in the assignment of the molecular geometry of these complexes, but the absence of complexes of higher stoichiometry seems to support the idea that the phenyl ring is included in the cavity and that the electrostatic repulsion between the protruding charged phenoxide moieties hampers the formation of 2:2 complexes. This is in agreement with the structure proposed for the complexes of 4-substituted phenols and phenolates with α-CD.[34] The association constants for the interaction of B-O$^-$ with the three CDs are reported in Table 2.

For both B-OH and its dissociated form, the association constants with β-CD at 20 °C $\pm$ 1 obtained on the basis of Equation (9) are $K \approx 6000\ M^{-1}$, an unusually high value for phenol-type compounds ($K \approx 100\ M^{-1}$ for phenol, $\approx 200\ M^{-1}$ for *p*-cresol[13, 35, 36]). Enthalpy and entropy of complexation calculated from the temperature dependence of the equilibrium constants, shown in Figure 11, are -14.0 ± 1.5 kJ mol^{-1} and 25 ± 5 J mol^{-1} K^{-1} for B-OH and -18.5 ± 2 kJ mol^{-1} and 10.5 ± 7 J mol^{-1} for B-O$^-$, respectively. These values should be compared with the values of ≈ -12.5 kJ mol^{-1} and ≈ 4 J mol^{-1} K^{-1} for phenol and *p*-cresol.[35] Thus both complexes have a binding energy comparable to that of simpler phenols, but the entropy change upon complexation is appreciably higher. The entropy of complexation can be related to the number of configurations of comparable energy available to the host–guest system.[35] One should conclude that the β-CD:B-OH complexes have appreciably more degrees of freedom than the complexes of β-CD with the more rigid molecules, phenol or *p*-cresol. A further contribution to the large complexation entropy could be due to hydrophobic interactions.[35, 37, 38]

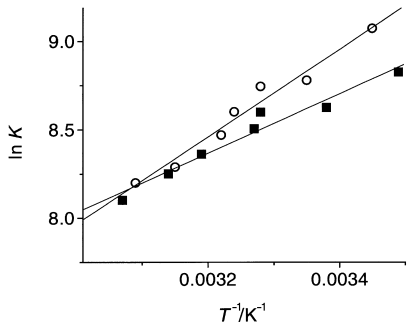

Figure 11. Temperature dependence of the equilibrium constant for the complexation of B-OH in 1 M HCl(■) and B-O$^-$ in 0.5 M phosphate buffer, pH 11.2 (○).

Lifetime measurements: The time-resolved fluorescence of B-OH was examined in 1 M HCl solution in the presence of variable [α-CD], up to 5×10^{-2} M, [β-CD], up to 3×10^{-3} M, and [γ-CD], up to 1×10^{-2} M. The solutions were excited at the isosbestic point in the absorption spectra of the free and complexed B-OH. The emission was observed at 335 nm, close to the maximum of the emission band. Global analysis of the decay curves at different CD concentrations gave a good description of the time profiles by deconvolution to a sum of three exponential terms with time constants independent of the CD concentration. Figure 12 summarizes the results. One

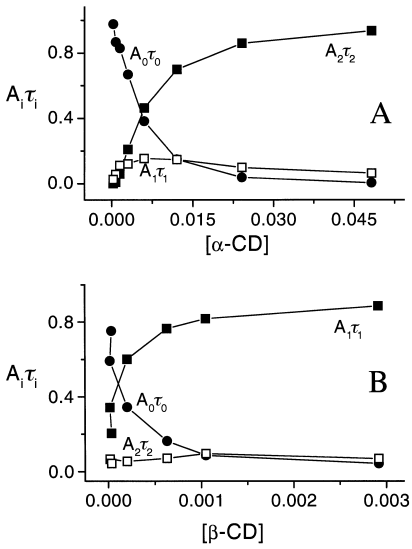

Figure 12. Integrated luminescence components from B-OH 2.2×10^{-5} M in 1 M HCl at different CD concentrations, extracted by global analysis of time profiles: **A**) α-CD, $\lambda_{exc} = 280$ nm, $\lambda_{em} = 335$ nm, $\tau_0 = 1.55$ ns, $\tau_1 = 4.3$ ns, $\tau_2 = 10.8$ ns ($\chi^2_g = 1.14$); **B**) β-CD, $\lambda_{exc} = 280$ nm, $\lambda_{em} = 335$ nm, $\tau_0 = 1.55$ ns, $\tau_1 = 7.3$ ns, $\tau_2 = 4.3$ ns ($\chi^2_g = 1.15$). $T = 295$ K.

of the time constants, $\tau_0 = 1.55$ ns, corresponding to the lifetime of the free molecule in solution, was fixed. Accordingly the relevant integrated emission intensity decreased with increasing CD concentration. The two additional longer-lived components in the emission are interpreted as due to the formation of inclusion complexes whose concentrations in the excited state are determined by the ground-state equilibria. The lifetimes of 4.3 ns and 10.8 ns, obtained in the presence of α-CD, are assigned to the 1:1 and 2:2 inclusion complexes,

0947-6539/00/0609-1586 $ 17.50+.50/0 *Chem. Eur. J.* **2000**, *6*, No. 9

respectively. By inspecting the concentration dependences of the corresponding integrated emission intensities, it is seen that the weight of the 1:1 complex, higher than that of the 2:2 at low [α-CD], increases with increasing [α-CD] up to 5×10^{-3} M and then decreases in agreement with the increasing concentration of the dimeric species which becomes by far predominant at high [α-CD]. Noticeably, the considerable lengthening of the lifetime in the 1:1 complex with respect to the free molecule (4.3 ns vs. 1.55 ns) can be only in part attributed to the protection against quenching by the acid[14] induced by the inclusion. In fact, the corresponding decrease of the F/F_0 values points to a decrease in the radiative decay parameter of the complex (see below).

With β-CD two complexed species of lifetimes 4.3 ns and 7.3 ns were determined. The contribution of the former is minor at any concentration and remains rather constant. The latter is assigned to the 1:1 complex on the basis of both the icd features and F/F_0 dependence on [β-CD], which are in agreement with the prevailing presence of a complex of this stoichiometry. The lifetime of 4.3 ns may tentatively be attributed to a 2:2 structure present in small traces, as suggested by the negative peak at 220 nm in the icd spectrum (Figure 2). This assignment is confirmed by the observation that the total emission intensity increases with increasing temperature, in agreement with the expected disfavoring of the dimeric structure. The low stability of the 2:2 complex, not predicted by the calculations, can be rationalized in the light of the thermodynamic features of the 1:1 complex. A large conformational flexibility about the central single bond, which would not be hindered by the inclusion in the large β-CD cavity, can be inferred for this complex on the basis of the important positive entropic term. This could prevent close stacking of the two phenyl rings, which is indicated by the calculations to be the driving force for the stabilization of the dimeric structure of the complex.

In the presence of γ-CD, in addition to the 1.55 ns lifetime of the free species, two components of 4.0 ns and 10.2 ns were observed and assigned to different complexed species. The intermediate component is major and is attributed to the 1:1 complex, because of the assessed predominance of this stoichiometry. As in the case of β-CD, a higher-order structure seems to be present in low concentration only.

At pH 11.2, the time-resolved fluorescence of B-O$^-$ was examined in the absence of CD and in the presence of 4.2×10^{-2} M α-CD, 7.0×10^{-3} M β-CD, and 3.0×10^{-2} M γ-CD, that is in the plateau region of the plot of the emission intensity versus [CD]. The emission wavelength was 400 nm, corresponding to the maximum of the fluorescence spectrum of B-O$^-$. The excitation was set at 287 nm.

In the presence of α-CD, a three-exponential decay with lifetimes 1.1 ns (to be compared with 0.95 ns found for the free B-O$^-$), 2.7 ns and 8.6 ns were observed, while in 0.1 M NaOH only two components with lifetime 0.9 ns and 1.9 ns were present. The third emitting species at pH 11.2 was attributed to the presence of a fraction of undissociated B-OH. To test this hypothesis, the excitation wavelength was increased to 300 nm and 310 nm where B-O$^-$ absorbs more efficiently than B-OH. It was found that the relative importance of the third component, $\tau = 8.6$ ns, decreases with increasing λ_{exc}. We conclude that this component is due to a complex of B-OH, probably the 2:2 structure on the basis of the long lifetime, and that the 2.7 ns component is due to a 1:1 B-O$^-$:α-CD complex.

In the presence of β-CD, the emission decay profiles are well described by a biexponential function with lifetimes 1.2 ns and 2.6 ns. These values should be compared with the values of 1.1 ns and 2.1 ns obtained in 0.1 M NaOH. From this analysis it can be safely concluded that B-O$^-$ gives a complex with β-CD of 1:1 stoichiometry and around 2 ns lifetime.

The emission decay profiles in the presence of γ-CD are also biexponential, with lifetimes 1.1 ns and 2.7 ns, attributed to the free B-O$^-$ and to the 1:1 complex, respectively.

Triplet state properties: The triplet–triplet absorption spectrum of neutral B-OH is characterized by a broad absorption band in the near UV, analogous to that of biphenyl.[39] Figure 13 shows the spectral properties of this band in a variety of cyclodextrin environments and in the neat solvents

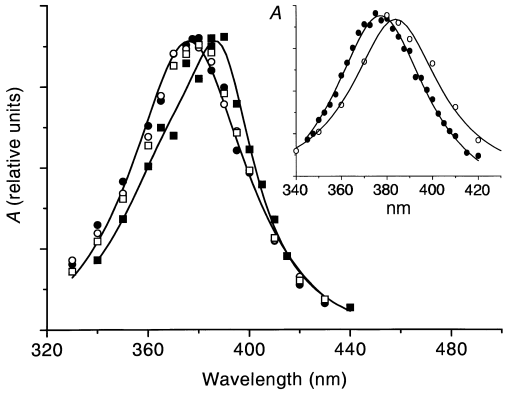

Figure 13. Triplet–triplet absorption spectra of B-OH in different environments at pH 2. (●) 0.005 M α-CD, (○) 5×10^{-4} M β-CD, (□) 0.01 M β-CD, (■) 0.05 M α-CD. Insert: (●) aqueous solution, (○) ethanolic solution.

H_2O and ethanol (displayed in the inset for comparison). A distinct blue shift of the band maximum is observed in H_2O ($\lambda_{max} = 377$ nm) as compared to ethanol ($\lambda_{max} = 384$ nm); a similar shift is observed in the ground state absorption spectra. The triplet–triplet spectrum in water is virtually unchanged by addition of low concentrations of α-CD (0.005 M) and low (5×10^{-4} M) as well as high (0.01 M) concentrations of β-CD. Increase of the concentration of α-CD to 0.05 M shifts λ_{max} to 386 nm and induces a slight asymmetry in the band shape. It may be hypothesized that the observed shifts are related to the hydrogen bond donor function of the B-OH hydroxy group toward H_2O which stabilizes the ground state as well as the lowest triplet state; this stabilization is absent in ethanol, and, by analogy, at high α-CD concentrations as well. Based on the fluorescence results, in this latter case the majority of B-OH molecules is included in the cyclodextrin host in the form of 2:2 complexes. It may therefore be assumed that the host–guest configuration adopted in the 2:2 complex prevents, at least partly, the formation of hydrogen bonds between the OH group and water molecules. The computed complex structures which seem to conform to this observation appear to be those in

which one, or both, OH groups are buried in the cavity interior (Figure 6, B, C).

The rate constants for triplet quenching by O_2 were measured in air-equilibrated solutions at temperatures ranging from 3 °C to 35 °C. Triplet decay is generally slower in presence of cyclodextrins than in neat aqueous solution; the effect of α-CD is much more pronounced than that of β-CD. Figure 14 shows the Arrhenius plots of the O_2 quenching rate constant in aqueous solution of B-OH at pH 2 and in presence

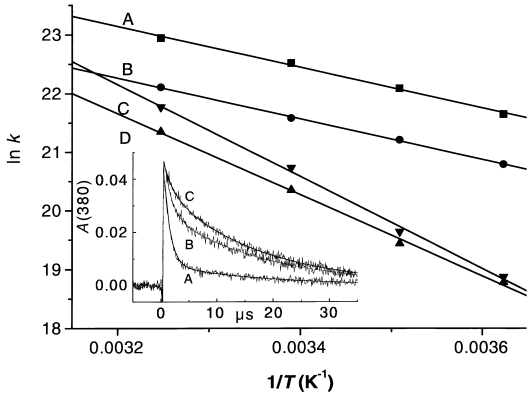

Figure 14. Arrhenius plots of the rate constant for the quenching of the triplet state of B-OH by O_2 at pH 2: A) in aqueous solution, B) with 0.01 M β-CD, C) with 0.02 M α-CD, D) with 0.05 M α-CD. Inset: Decay traces of the triplet–triplet absorption in solutions containing A) 0.002 M, B) 0.005 M, and C) 0.0075 M α-CD (pH 2, 278 K).

of high concentrations of β-CD (0.01 M) and of α-CD (0.02 M and 0.05 M), corresponding to 1:1 complexes with β-CD and 2:2 complexes with α-CD; at these concentrations, these structures are formed to a high degree (>90 %) in the temperature range shown. The activation energies determined for the aqueous and the β-CD environments are virtually equal (29.9 kJ mol^{-1} for H_2O and 30.0 kJ mol^{-1} for β-CD); these values are in the range expected for a diffusion-controlled reaction in an aqueous solution.[40] The rate constants for the β-CD-complexed B-OH are smaller than those in neat aqueous solution by a factor of about 2.5 over the whole temperature interval. In contrast, the 2:2 complex of triplet B-OH with α-CD reacts much more slowly with O_2, but at the same time, the activation energy is about doubled (65.8 kJ mol^{-1} for 0.02 M α-CD and 59.8 kJ mol^{-1} for 0.05 M α-CD). Both effects are in line with the assumption that the B-OH guest molecules are significantly better shielded from the aqueous bulk in the α-CD complex than in β-CD complex, in full agreement with the preceeding discussion based on the structure computation and the fluorescence measurements. The higher activation energy in the 2:2 complex with α-CD can be taken as the signature of a further activated process besides O_2 diffusion, which quite probably is related to the conformational flexibility of the complex. We may note at this point that neither the triplet–triplet absorption nor the triplet decay kinetics gave any hint of a change of complex stoichiometry in the triplet state with respect to the ground state.

The triplet decay kinetics could be fitted, within the experimental error, to a sum of two exponential components at cyclodextrin concentrations lower than those required for full complexation. This is exemplified in the inset of Figure 14, displaying experimental triplet–triplet absorption measurements in the presence of varying concentrations of α-CD (0.002 M, 0.005 M, and 0.0075 M) at 5 °C; the full lines are results of two-exponential fits, yielding values of the decay rate of 9.1×10^5 s^{-1}, 7.7×10^5 s^{-1}, and 6.0×10^5 s^{-1} for the fast component, and 6.1×10^4 s^{-1}, 5.8×10^4 s^{-1}, and 6.1×10^4 s^{-1} for the slow component (at the three mentioned concentrations of α-CD). The progressively decreasing values found for the fast component are probably due to the presence of the 1:1 complex; the relative contributions of the free B-OH and of the 1:1 complex to the decay could not be resolved.

Intersystem crossing quantum yields of B-OH in different environments were determined by triplet yield measurements, taking the value in ethanol solution as a reference. The latter was obtained by triplet energy transfer to anthracene ($\Phi_{ISC} = 0.7$[41]) with the result φ_{ISC} (B-OH) $= 0.87 \pm 0.05$. Experimental results on the pulse energy dependence of the triplet–triplet absorbance of B-OH are shown in Figure 15. The data

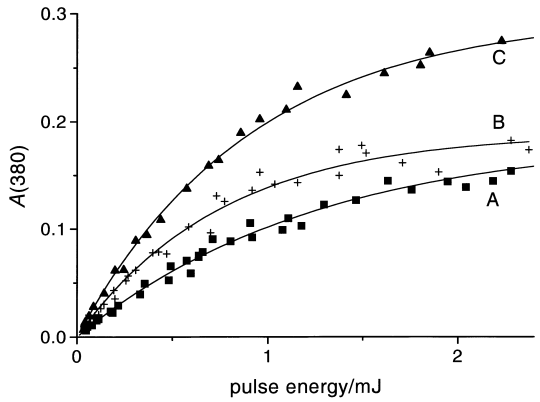

Figure 15. Dependence of the triplet–triplet absorption, measured at 380 nm (pH 2, 295 K), on laser pulse energy. A) in aqueous solution, B) with 0.005 M β-CD, C) with 0.05 M α-CD.

show a characteristic saturation behavior due to ground-state depletion, which is basically governed by Equation (10) where c_T is the concentration of triplet states, c_0 the total B-OH concentration, ε_T the triplet–triplet extinction coefficient, Φ_{ISC} the intersystem crossing yield, and I the laser photon fluence (proportional to the pulse energy).[20]

$$c_T = c_0 \times \exp(-2.303 \times \varepsilon_T \times \varepsilon_{ISC} \times I) \quad (10)$$

According to Equation (10), the low-fluence slope of the curve depends on the product $\varepsilon_T \times \Phi_{ISC}$, whereas the plateau value at high fluence permits the determination of ε_T, since $c_T = c_0$ then holds. However, the high fluence behavior of actual systems is very often more complex, especially if the fluorescence lifetime of the molecule in question is not negligibly short compared with the laser pulse duration,[42] or if there is notable fluence-dependent (e.g., two-photon) photochemistry. Both effects tend to reduce the measured plateau value with respect to that predicted by Equation (10). Therefore, only the product $\varepsilon_T \times \varphi_{ISC}$ can usually be deter-

0947-6539/00/0609-1588 $ 17.50+.50/0 Chem. Eur. J. 2000, 6, No. 9

Table 3. Radiative and nonradiative deactivation rate parameters of B-OH, B-O$^-$ and their inclusion complexes with α-, β-, and γ-CD.

	φ_F[a]	φ_{ISC}[e]	τ_F/ns[d]	k_r/s^{-1}	k_{ISC}/s^{-1}	k_{IC}/s^{-1}	k_{nr}/s^{-1}
B-OH:β-CD (1:1)	0.18	0.78	7.3	2.5×10^7	1.1×10^8		1.1×10^8
B-OH:γ-CD (1:1)	0.12		4.0	3.0×10^7			2.2×10^8
B-OH:α-CD (1:1)	(0.007)[b]		4.3	(1.6×10^6)[b]			(2.3×10^8)[b]
B-OH:α-CD (2:2)	(0.4)[c]	($\geq$0.25)	10.8	(3.7×10^7)[c]	($\geq2.3\times10^7$)		(5.5×10^7)[b]
Free B-OH	0.075	0.52	1.55	4.8×10^7	3.3×10^8	2.7×10^8	6.0×10^8
B-O$^-$:β-CD (1:1)	0.18		2.1	8.6×10^7			3.9×10^8
B-O$^-$:γ-CD (1:1)	0.16		2.7	5.9×10^7			3.1×10^8
B-O$^-$:α-CD (1:1)	0.095		1.9	5.0×10^7			4.8×10^8
Free B-O$^-$	0.065		0.95	6.8×10^7			9.8×10^8

[a] Uncertainty $\pm10\%$. [b] This value has to be taken as only indicative (see Table 2 and text). [c] This value results from fixing the quantum yield ratio of the 2:2 complex (see Table 2 and text). [d] Estimated uncertainty within $\pm7\%$. [e] Uncertainty $\pm15\%$.

mined in such a measurement; all the same, the obtained plateau values allow a qualitative comparison between different types of B-OH – cyclodextrin complexes.

Comparing in Figure 15 the results obtained in aqueous solution of B-OH (A) and in presence of 0.005 M β-CD (B), it is noted that the initial slope of the plots is higher in the second case, but the plateau values converge to a similar limiting value. This is consistent with the assumption that the triplet – triplet extinction coefficients of the free molecule and of the 1:1 complex with β-CD are similar. Consequently, Φ_{ISC} must be assumed to be higher in the complex; the values deduced from the initial slopes are $\Phi_{ISC}=0.52$ for the free molecule in aqueous solution and $\Phi_{ISC}=0.78$ for the β-CD complex, both based on the value in ethanolic solution mentioned above under the assumption that ε_T remains constant.

In the presence of 0.05 M α-CD (Figure 15, C), both the initial slope as well as the plateau value are significantly increased, the enhancement factors with respect to the aqueous solution being 2.2 and 1.6. This result cannot be simply explained by assuming an increase of ε_T in the complex, since the sum of fluorescence and intersystem crossing quantum yields would then be well above 1; indeed, the large enhancement of Φ_F in the α-CD complex (see Figure 9 and 10) do not leave room for a comparable increase of Φ_{ISC}. One possible solution to this apparent contradiction is to assume that the spectroscopic properties of the triplet state are altered by the close contact of the two chromophores in the 2:2 complex. Assuming that the interaction between the two B-OH moieties in the complex is strong (and might actually be stronger than in the ground state due to planarization of the molecules), it would be more appropriate to consider the system as consisting of B-OH dimers exhibiting twice the oscillator strength, that is four times the extinction coefficient of the monomer. As the concentration would be halved at the same time, a doubling of the plateau values in Figure 15 would be expected. The actual enhancement factor is only 1.6; this could be due to the longer fluorescence lifetime of the 2:2 complex and a corresponding reduction of the plateau value.[42] Within this model, the value of ε_T can thus assumed to lie between values corresponding to 3.2 and four times the value of the monomer. Consequently, the intersystem crossing yield for the 2:2 complex is set to $0.32\geq\Phi_{ISC}\geq0.25$. This conclusion, based on the experimental evidence shown in Figure 15, allows to reach a consistent picture of the excited state deactivation pathways of the complex.

Photophysical parameters: Table 3 reports the emission quantum yields of B-OH in 1 M HCl, of B-O$^-$ in 0.1 M NaOH, and those of the complexed species calculated on the basis of the Φ_b/Φ_0 values of Table 2. The experimental lifetimes and the calculated photophysical parameters, $k_r=\Phi_F/\tau$ and $k_{nr}=1/\tau-k_r$ are also reported.

In the β- and γ-CD 1:1 complexes of B-OH a decrease of both the radiative and nonradiative rate constants with respect to the values of the free molecule is observed. In the β-CD complex the nonradiative channel is essentially intersystem crossing, so that a drastic reduction of the internal conversion efficiency can be inferred. Steric hindrance by the cavity interactions to the high energy modes assisting the $S_1\rightarrow S_o$ nonradiative deactivation, especially the CH and the ring modes, can be reasonably suggested on the basis of the complex structure reported in Figure 5. The lowering of k_r also reflected by the lower intensity of the absorption spectra in the presence of CD, can be associated to the effect of the inclusion on the torsional mode about the central single bond. It is known that this mode plays a key role in the emission behavior of biphenyl derivatives which are nonplanar in the ground state and tend to become planar in the excited state.[18, 43] Steric hindrance to attain the planar conformation could therefore directly influence the emission probability. The decrease of k_r is more than compensated by the decrease of k_{nr}, so that a net increase of the fluorescence quantum yield is observed. For the same reason Φ_{ISC} sensibly increases, despite a reduction of a factor around 3 of the ISC rate constant.

Quantitative estimate of the rate parameters of the α-CD complexes is more delicate. As mentioned, the parameters relevant to the 2:2 complex in Equation (7) were fixed to reproduce the plateau in Figure 10. The fluorescence quantum yield was therefore assumed to be about 0.4 and the association constant about 75 000 M^{-1}. We notice that an emission quantum yield for the 2:2 complex sensibly higher than that of the free molecule is in agreement with the tenfold increase of the fluorescence lifetime and that the above value is consistent with the value of $\Phi_{ISC}\cong0.25-0.32$. Despite these assumptions the parameters relevant to the 1:1 complex still are not completely determined by the least-square fitting procedure (i.e., different solutions have similar χ^2 values). However, the best solutions (like that represented in Figure 10) correspond to association constants of the order of 100 M^{-1}, consistent with literature results for a substituted phenyl ring interacting with the α-CD cavity,[12, 32, 33] and an

emission quantum yield lower than that of the free molecule at least by one order of magnitude. This result is in agreement with the decrease in the emission intensity observed at low α-CD concentrations. By taking into account that the lifetime of this species is by a factor three longer, it is inferred that its k_r is drastically decreased. The conformation of the 1:1 complex does not show a deep penetration of the guest in the cavity, see Figure 5, so that a severe hindrance to the torsional mode is not expected. A change in the molecular symmetry in the associated structure leading to a less allowed, more biphenyl-like S_1 state by weakening of the substituent perturbation on the lowest excited singlet, can be hypothesized. The lengthening of the S_1 lifetime, indicating a change of the -OH group environment, is in agreement with this hypothesis.

The tenfold increase of the emission lifetime in the dimer appears to be largely due to a decrease of k_{nr}, the k_r value remaining the same as in the monomer. A drastic reduction of the proton dissociation rate is supported by the spectral modification of the emission by increasing [α-CD] and by the equilibrium conformation of the complex, in which at least one of the OH groups is buried in the cavity.

In the 1:1 complexes of B-O^- with the three cyclodextrins the increase of the fluorescence quantum yields is also accounted for by a decrease of k_{nr} (Table 2). Charge migration from the O^- group towards the benzene ring should make the anion more planar with respect to the neutral B-OH (as found for the biphenyl anion[44]). Excitation increases the charge delocalization so that no important conformational changes are expected upon relaxation in S_1. Thus the effect on k_{nr} can be generically attributed to the limitation of the molecular mobility, while the lack of an effect on k_r indirectly confirms a role of the torsional degree of freedom for the radiative deactivation of the neutral molecule.

Conclusions

The structural, spectroscopic and photophysical properties of host–guest inclusion complexes of 4-OH-biphenyl with cyclodextrins have been investigated using an array of computational and spectroscopic techniques. The results of the present study demonstrate that this approach, which we have applied before on a variety of other cyclodextrin complexes[12c,13, 25–27] has the potential to provide a detailed picture of the behavior of complexes involving a guest molecule which is asymmetric, flexible, and able to undergo a prototropic dissociation reaction.

Among the cyclodextrins used as hosts, γ-CD presents the least interesting case. The fluorescence data are consistent with the formation of weak 1:1 complexes. Due to the large cavity dimensions, the prototropic equilibrium is not influenced, but there is a reduction in the nonradiative deactivation rate with respect to the free guest molecule by about a factor of three.

The two smaller cyclodextrins form significantly stronger complexes with a much more varied behavior. The experimental data obtained on the B-OH–β-CD system concur to show that 1:1 complexes are the dominant form over a broad range of CD concentrations, covering more than two orders of magnitude. This configuration is characterized by a high degree of conformational flexibility, which is reflected in an unusually large entropic contribution to the free energy of complexation and a correspondigly high association constant. The OH group remains accessible to the aqueous environment; both the prototropic equilibrium and the quenching of the triplet state by O_2 are accordingly little influenced. Based on the computational prediction, both 1:2 and 2:2 B-OH–β-CD configurations are energetically favored. Formation of 1:2 complexes can be ruled out on the basis of the circular dichroism data; 2:2 complexes may be responsible for a minor component present in the fluorescence decay, but would have to be assumed to be unstable. The photophysical properties of the 1:1 complex are characterized by a virtually total suppression of internal conversion and a concomitant increase of both fluorescence and intersystem crossing quantum yields.

The dominant feature of the B-OH–α-CD system is the formation of 2:2 complexes. A detailed examination of the dependence of both fluorescence intensity and lifetimes of B-OH on the concentration of α-CD allowed the characterization of the consecutive formation of 1:1 and 2:2 complexes in terms of association constants. The 2:2 complexes feature an array of distinctive spectroscopic and photophysical properties, including a characteristic circular dichroism, increased fluorescence quantum yield and lifetime, and a substantial red-shift of the triplet–triplet absorption. The latter is consistent with the suppression of the hydrogen bond donor ability of the hydroxy group of the guest, suggesting efficient shielding from the aqueous environment. This conclusion is fully supported by the observations of significantly reduced prototropic dissociation on one hand, and hindered triplet quenching by O_2 on the other. The calculations predict, in particular, energetically favored conformations in which one, or both, guest OH groups are buried in the cavity interior. An unequivocal preference for one of these two possibilities could not be achieved. Both cases present, however, good examples for the assembly of a supramolecular structure requiring both host–host and guest–guest interaction. The guest–guest interaction is particularly manifest in the triplet state, which based on its spectroscopic behavior has to be viewed as a strongly coupled dimer.

[1] M. L. Bender, M. Komiyama, *Cyclodextrin Chemistry*, Springer, Berlin, **1978.**

[2] J. Szejtli, *Cyclodextrins and Their Inclusion Complexes*, Akademiai Kiado, Budapest, **1982**.

[3] V. Balzani, L. De Cola, *Supramolecular Chemistry*, Kluwer, Dordrecht, **1992**.

[4] P. Bortolus, S. Monti, *Adv. Photochem.* **1996**, *21*, 1–133.

[5] a) N. Kobayashi, R. Saito, Y. Hino, A. Ueno, T. Osa, *J. Chem. Soc. Chem. Commun*. **1982**, 706–707; b) T. Tamaki, *Chem. Lett*. **1984**, 53–56; c) T. Tamaki, T. Kokubu, *J. Incl. Phenom*. **1984**, *2*, 815–822; d) M. Ohashi, K. Kasatani, H. Shinohara, H. Sato, *J. Am. Chem. Soc*. **1990**, *112*, 5824–5830.

[6] a) N. Kobayashi, R. Saito, H. Hino, Y. Hino, A. Ueno, T. Osa, *J. Chem. Soc. Perkin Trans. II* **1983**, 1031–1035; b) S. Hamai, *J. Phys. Chem*. **1989**, *93*, 6527–6529; c) V. Pushkara Rao, N. J. Turro, *Tetrahedron Lett*. **1989**, *30*, 4641–4644; d) V. Buss, *Angew. Chem.* **1991**, *103*, 889–890; *Angew. Chem. Int. Ed. Engl*. **1991**, *30*, 869–870; d) A. Nakamura, S. Sato, K. Hamasaki, A. Ueno, F. Toda, *J. Phys. Chem*. **1995**, *99*, 10952–10959.

0947-6539/00/0609-1590 $ 17.50+.50/0 *Chem. Eur. J.* **2000**, *6*, No. 9

[7] X. Shen, M. Belletête, G. Durocher, *J. Phys. Chem. B* **1998**, *102*, 1877–1883.
[8] a) A. Harada, J. Li, M. Kamachi, *Nature* **1992**, *356*, 325–327; b) A. Harada, J. Li, M. Kamachi, *Nature* **1994**, *370*, 126–128; c) B. Mayer, C. T. Klein, I. N. Topchieva, G. Köhler, *J. Comput. Aided Mol. Des.* **1999**, *13*, 373–383.
[9] V. Ramamurthy, *Tetrahedron* **1986**, *42*, 5753–5839.
[10] a) N. Chattopadhyay, T. Chakraborty, A. Nag, M. Chowdhury, *J. Photochem. Photobiol. A*: *Chem*. **1990**, *52*, 199–204; b) N. Chattopadhyay, *J. Photochem. Photobiol. A*: *Chem*. **1991**, *58*, 31–36; c) N. Chattopadhyay, R. Dutta, M. Chowdhury, *Indian J. Chem*. **1992**, *31A*, 512–517.
[11] J. E. Hansen, E. Pines, G. R. Fleming, *J. Phys. Chem*. **1992**, *96*, 6904–6910.
[12] a) T. Yorozu, M. Hoshino, M. Imamura, H. Shizuka, *J. Phys. Chem*. **1982**, *86*, 4422–4426; b) D. F. Eaton. *Tetrahedron* **1987**, *43*, 1551–1570; c) H.-R. Park, B. Mayer, P. Wolschann, G. Köhler, *J. Phys. Chem*. **1994**, *98*, 6158–6166.
[13] S. Monti, G. Köhler, G. Grabner, *J. Phys. Chem*. **1993**, *97*, 13011–13016.
[14] R. Townsend, S. G. Schulman, *Chimica Oggi* **1992**, *10*, 49–52.
[15] H. H. Jaffé, M. Orchin in *Theory and Applications of Ultraviolet Spectra*, Wiley, New York, **1962**, pp. 397–407.
[16] L. S. Rosenberg, G. Lam, G. Groh, S. G. Schulman, *Anal. Chim. Acta* **1979**, *106*, 81–87.
[17] A. Muñoz de la Peña, A. Fernández Gutiérrez, S. G. Schulman, *Anal. Lett.* **1985**, *18*, 2489–2495.
[18] a) H. Suzuki, *Bull. Chem. Soc. Jpn*. **1959**, *32*, 1340–1350; b) T. Fujii, S. Suzuki, S. Komatsu, *Chem. Phys. Lett*. **1978**, *57*, 175–178; c) T. Fujii, S. Komatsu, S. Suzuki, *Bull. Chem. Soc. Jpn*. **1982**, *55*, 2516–2520; d) H.-S. Im, E. R. Bernstein, *J. Chem. Phys.* **1988**, *88*, 7337–7345.
[19] a) J. M. Bello, R. J. Hurtubise, *Anal. Chem*. **1987**, *59*, 2395–2400; b) J. M. Bello, R. J. Hurtubise, *Appl. Spectrosc*. **1988**, *42*, 619–623.
[20] G. Grabner, N. Getoff, T. Gantchev, D. Angelov, M. Shopova, *Photochem. Photobiol*. **1991**, *54*, 673–681.
[21] N. L. Allinger, Y. H. Yuh, J. H. Lee, *J. Am. Chem. Soc*. **1989**, *111*, 8551–8566.
[22] C. Betzel, W. Saenger, B. E. Hingerty, G. M. Brown, *J. Am. Chem. Soc*. **1984**, *106*, 7545–7557.
[23] a) N. Metropolis, A. W. Rosenbluth, M. B. Rosenbluth, A. H. Teller, *J. Chem. Phys.* **1953**, *21*, 1087–1092; b) S. Kirkpatrick, C. D. Gelatt, M. P. Vecchi, *Science* **1983**, *220*, 671–680.
[24] Program Package MultiMize, B. Mayer, Vienna, Austria **1997**.
[25] B. Mayer, G. Marconi, C. T. Klein, G. Köhler, *J. Incl. Phenom. Molec. Recogn. Chem*. **1997**, *29*, 79–93.
[26] G. Grabner, S. Monti, G. Marconi, B. Mayer, C. T. Klein, G. Köhler, *J. Phys. Chem*. **1996**, *100*, 20068–20075.
[27] G. Marconi, B. Mayer, C. T. Klein, G. Köhler, *Chem. Phys. Lett*. **1996**, *260*, 589–594.
[28] I. Tinoco, Jr., *Adv. Chem. Phys.* **1962**, *4*, 113–160.
[29] J. A. Schellman, *Acc. Chem. Res.* **1968**, *1*, 144–151.
[30] M. T. Beck, in *Chemistry of Complex Equilibria*, Van Nostrand, New York, **1970**, ch. 5.
[31] K. A. Connors, *Chem. Rev.* **1997**, *97*, 1325–1357, and references therein.
[32] M. Kamiya, S. Mitsuhashi, M. Makino, H. Yoshioka, *J. Chem. Phys.* **1992**, *96*, 95–99.
[33] D. W. Cho, Y. K. Kim, S. G. Kang, M. Yoon, *J. Phys. Chem.* **1994**, *98*, 558–562.
[34] S.-F. Lin, K. A. Connors, *J. Pharm. Sci*. **1983**, *72*, 1333–1338.
[35] G. L. Bertrand, J. R. Faulkner, Jr., S. M. Han, D. W. Armstrong, *J. Phys. Chem*. **1989**, *93*, 6863–6867.
[36] M. V. Rekharsky, Y. Inoue, *Chem. Rev*. **1998**, *98*, 1875–1917.
[37] W. C. Cromwell, K. Bystrom, M. R. Eftink, *J. Phys. Chem*. **1985**, *89*, 326–332.
[38] M. R. Eftink, M. L. Andy, K. Bystrom, H. D. Perlmutter, D. S. Kristol, *J. Am. Chem. Soc*. **1989**, *111*, 6765–6772.
[39] I. Carmichael, G. L Hug., *J. Phys. Chem. Ref. Data* **1986**, *15*, 1–250.
[40] D. Eisenberg, W. Kauzmann, *The Structure and Properties of Water*, Clarendon Press, Oxford, **1969**, p. 205.
[41] B. Amand, R. Bensasson, *Chem. Phys. Lett*. **1975**, *34*, 44–48.
[42] a) G. L. Hug, I. Carmichael, *J. Photochem*. **1985**, *31*, 179–192; b) I. Carmichael, G. L. Hug, *J. Phys. Chem*. **1985**, *89*, 4036–4039.
[43] E. C. Lim, and Y. H. Li, *J. Chem. Phys.* **1970**, *52*, 6416–6422.
[44] K. Razi Naqvi, J. Donatch, U. P. Wild, *Chem. Phys. Lett.* **1975**, *34*, 285–288, and references therein.

Received: July 1, 1999 [F 1889]